Elastic Moduli of Hardened Portland Cement and Tricalcium Silicate Pastes: Effect of Porosity

RICHARD A. HELMUTH, Research Physicist, and
DANICA H. TURK, Associate Research Chemist, Basic Research Section, Portland Cement Association

A resonance frequency method was developed for use with thin (1-2 mm thickness) slabs of hardened pastes. Elastic moduli calculated from the resonance frequencies were strongly porosity dependent; Poisson's ratio was not. The elastic moduli are found to vary as $(1-\epsilon)^3$ where ϵ is the porosity. This relationship is obtained from consideration of the porosity of the paste.

•AN UNDERSTANDING of such important properties of concrete as elasticity, creep and drying shrinkage requires knowledge of the elastic moduli of the hardened portland cement paste binder. The elastic moduli of hardened portland cement pastes depend on both the porosity and the elastic moduli of the constituent solid phases. The solid phases include some crystalline phases, but the major constituent is the cement gel, a poorly crystallized material with a high specific surface area. Studies of portland cement pastes and pure calcium silicate hydrates indicate that this gel is composed of porous aggregations of small particles (1, 2). Direct measurement of the moduli of the particles cannot be made because of their small sizes.

The objectives of the present work are to determine the elastic moduli of hardened pastes over their normal range of porosities, and to develop relationships between the elastic moduli of the pastes and their porosities. The average moduli of the solids can then be obtained from the values of the moduli of the pastes as the porosity approaches zero. Elastic moduli calculated from resonance frequencies of thin slabs (1-2 mm thickness) of hardened pastes have been found to agree well with an empirical equation (see Eq. 8 below) introduced by Powers (3). Of the various empirical and theoretical equations which have been published only this equation and one given by Hansen (4) were found to fit our data. Hansen's equation is a modification of a theoretical equation derived by Hashin (5). This modification is obtained by introducing a factor that reduces the calculated moduli. The effect of this factor is so great that the modified equation can hardly be regarded as being based on the same theory. Furthermore, although the modified equation is of slightly different form it gives essentially the same results as Powers' equation in the porosity range that can be obtained. We have therefore chosen to compare our data with Powers' equation because of its simpler form.

EXPERIMENTAL METHODS

Original Materials

Three different materials were used to prepare the hardened paste specimens. Two were portland cements designated by the numbers 15366 and 15754, with specific surface areas of 4470 and 3420 cm^2/g Blaine (6), respectively. The third was a nearly pure tricalcium silicate of 4410 cm^2/g specific surface area. The compositions of these materials are given in Table 1.

Hardened Pastes

To obtain specimens free of air voids, pastes of water and cement were mixed in vacuo. Two different methods were used. In the first method mixing was done in a Waring Blendor under an evacuated bell jar (7). In the second method the pastes were

TABLE 1

COMPUTED COMPOUND COMPOSITION OF ORIGINAL MATERIALS (PERCENT)

Component	Tricalcium Silicate	Cement 15366	Cement 15754
C_3S	100	46.7	46.5
C_2S	—	24.9	24.3
C_3A	—	12.7	12.4
C_4AF	—	8.2	8.2
$CaSO_4 \cdot 2H_2O$	—	3.3	4.0
Loss on ignition	—	0.77	0.92
MgO	—	2.6	2.5
Total alkali	—	0.33	0.33
Specific surface (cm^2/g)	4410	4470	3420

mixed by shaking in an evacuated cell mounted in a commercial shaker ("paint conditioner") at 120 cps for 3 min. The molds, polyethylene boxes 105 by 27 by 115 mm high, were vibrated on a vibrating table during casting. After casting, the paste was covered with added water to insure saturation during curing. The molds were kept tightly closed until the end of the curing period.

At the end of the curing period the block of hardened paste was removed from the mold and trimmed and cut into three sections measuring about 15 by 80 by 30 mm with a rough-duty diamond saw. Inhomogeneous regions, such as those near the surfaces of the original block, were cut away and discarded. At the same time companion pieces used for total water content and density determinations were cut from the blocks immediately adjacent to the sections from which the thin slabs were to be cut.

Thin Slab Specimens

A thin-sectioning machine was used to cut the sections into thin-slab specimens measuring about 15 by 80 by 1 (or 2) mm. The slabs were cut horizontally (as cast) from the sections to minimize the gradients in density that result from sedimentation of cement particles in the fresh paste (8). The samples were kept wet during all operations. However, to avoid excessive leaching of calcium hydroxide the thin slabs were not exposed to large volumes of water for long periods of time.

Measurements of length, width, thickness, and mass of the water-saturated thin slabs were made in a glove box at 25 C. Water-saturated CO_2-free air was supplied to the glove box under slight positive pressure. Three determinations of the length and width of each thin slab specimen were made with a vernier caliper (±0.1 mm). Six determinations of the thickness of each thin slab were made with a Hamilton dial indicator (±0.002 mm) in a comparator stand with flat anvil. The uniformity of thickness was usually ±0.01 mm. The measurements were made at regular intervals along the slab to obtain a representative measurement of each dimension. The mass of each specimen was determined by weighing on an analytical balance.

Composition of the Hardened Pastes

The nonevaporable water, w_n, of the paste in each section was obtained from the loss on ignition of thin slabs which had been dried in vacuum in apparatus essentially like that used by Copeland and Hayes (9). The thin slabs were weighed weekly during the drying period (usually about six weeks) until the rate of weight loss decreased to about 0.3 mg/g of sample per day. Then 1-gram samples were ignited at 1050 C to constant weight. This procedure gives results that are not significantly different from those determined by the method of Copeland and Hayes.

The densities of the thin slabs were calculated directly from the mass and dimensions of the wet slabs. The density of each companion piece was determined by weighing in water and in air.

The total water content, w_t, and the ignited weight, c_i, of the saturated companion pieces were calculated directly from the loss on ignition at 1050 C. This loss on ignition, w_t/c_i, of each slab was not exactly the same as that of the companion pieces because of slight differences in porosity and density caused by sedimentation of the cement particles in the fresh paste. A more accurate average value of w_t/c_i of each thin slab was determined in the following way. First the w_t/c_i of the companion pieces was plotted against their densities; the points for each set of specimens determined a well defined curve. This curve was then used to obtain the w_t/c_i of each thin slab from its density, ρ.

Leaching of the alkalies present in the portland cement paste slabs during wet handling was in all cases large, and in some cases nearly complete, as indicated by flame photometric analyses. Leaching of calcium hydroxide was not appreciable, as indicated by CaO and SiO_2 analyses.

Calculation of Porosity

The total porosity, ϵ_t, of each thin slab was calculated from

$$\epsilon_t = \frac{v_e(w_t - w_n)\rho}{w_t + c_i} \tag{1}$$

in which v_e is the specific volume of the evaporable water, $w_t - w_n$. In all calculations v_e was taken to be unity.

The capillary porosity, ϵ_c, was calculated for the cement pastes according to

$$\epsilon_c = \frac{v_c(w_t - 1.74\, w_n)\rho}{w_t + c_i} \tag{2}$$

The value of the specific volume of the capillary water, v_c, was also taken to be unity. Eqs. 1 and 2 were given in slightly different form by Copeland and Hayes (10). For the tricalcium silicate pastes the constant 1.74 in this equation was replaced by 1.64 because the porosity of the gel in tricalcium silicate pastes was found to be lower than that in portland cement pastes. The value of this constant was determined by the same method used by Copeland and Hayes (10) for portland cement pastes.

Resonance Frequency Measurements

Measurements of the fundamental flexural and torsional resonance frequencies of thin-slab specimens were made in CO_2-free air of controlled humidity in a glove box at 25 C. The method used was that described by Spinner and Tefft (11), modified to the requirements of the thin-slab specimens. Several kinds of suspension systems were tried. Best results were obtained with the thin slab supported near a node and vibrated

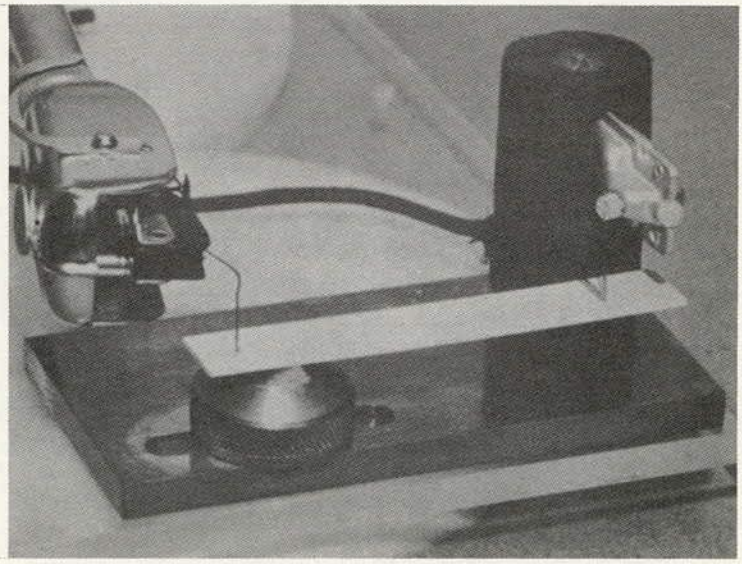

Figure 1. Apparatus used in determination of resonance frequencies of thin slab specimens.

by a wire clip driven by a crystal phonograph cartridge. The other end of the thin slab was supported at a node by a soft foam plastic pad. The vibration was detected by a wire probe cemented to a Sonotone 3P-1S ceramic cartridge. The cartridge was mounted in a modified Rek-o-Cut S-320 tone arm. The stylus pressure was adjusted to the minimum required to maintain contact between the specimen and probe. The arrangement is shown in Figure 1.

At least three measurements of each resonance frequency were made, changing the positions of the supports between each measurement. The precision was about ±5 cps per 1000 cps. Resonance frequencies ranged from about 250 cps to 4000 cps.

RESULTS

Tables 2, 3, and 4 give the density, w_t/c_i and w_n/c_i values of each water-saturated, thin-slab specimen. Also listed are the total and capillary porosities calculated from Eqs. 1 and 2.

The fundamental resonance frequencies in flexure, f_f, and in torsion, f_t, of the water-saturated, thin-slab specimens were used to calculate the Young's modulus, E, and shear modulus, G, from the following equations (11):

$$E = 0.94642 \frac{\rho\, l^4\, f_f^2}{a^2}\, T \tag{3}$$

$$G = 4\, \rho\, l^2\, f_t^2\, R_o \tag{4}$$

TABLE 2

DATA FOR WATER-SATURATED SPECIMENS OF TRICALCIUM SILICATE B-101 PASTES MOIST CURED 8 AND 14 MONTHS

Density (g/cc)	w_t/c_i (g/g)	w_n/c_i (g/g)	ϵ_t	ϵ_c	E × 10^{-6} (psi)	G × 10^{-6} (psi)	ν	K × 10^{-6} (psi)
Cured 8 Months								
1.8038	0.641	0.205	0.479	0.335	2.09	0.82	0.271	1.53
1.8247	0.622	0.205	0.469	0.332	2.20	0.87	0.263	1.56
1.8729	0.579	0.204	0.445	0.291	2.50	0.99	0.258	1.72
1.9016	0.554	0.204	0.428	0.269	2.66	1.05	0.269	1.92
2.0952	0.389	0.175	0.323	0.155	4.17	1.64	0.269	3.03
2.1279	0.368	0.175	0.300	0.127	4.38	1.76	0.248	2.91
Cured 14 Months								
2.2410	0.300	0.176	0.214	0.021	5.33	2.03	0.310	4.67
2.2448	0.298	0.176	0.211	0.017	5.26	2.01	0.307	4.56
2.2498	0.295	0.176	0.207	0.012	5.39	2.12	0.279	4.07

TABLE 3

DATA FOR WATER-SATURATED SPECIMENS OF PORTLAND CEMENT 15366 PASTES MOIST CURED 14 MONTHS

Density (g/cc)	w_t/c_i (g/g)	w_n/c_i (g/g)	ϵ_t	ϵ_c	E × 10^{-6} (psi)	G × 10^{-6} (psi)	ν	K × 10^{-6} (psi)
1.6627	0.858	0.234	0.558	0.404	1.01	0.46	—	0.42
1.6673	0.853	0.234	0.557	0.401	1.01	0.40	0.264	0.71
1.8170	0.668	0.234	0.473	0.284	1.61	0.66	0.219	0.95
1.8204	0.664	0.234	0.470	0.281	1.66	0.63	0.306	1.43
2.0297	0.479	0.223	0.351	0.125	3.00	1.17	0.284	2.32
2.0309	0.478	0.223	0.350	0.124	2.94	1.19	0.235	1.85
2.1692	0.376	0.203	0.273	0.036	4.10	1.57	0.310	3.60
2.1921	0.361	0.203	0.254	0.013	4.19	1.67	0.257	3.14

TABLE 4

DATA FOR WATER-SATURATED SPECIMENS OF PORTLAND CEMENT 15754 PASTES MOIST CURED 6, 7 AND 24 MONTHS

Density (g/cc)	w_t/c_i (g/g)	w_n/c_i (g/g)	ϵ_t	ϵ_c	$E \times 10^{-6}$ (psi)	$G \times 10^{-6}$ (psi)	ν	$K \times 10^{-6}$ (psi)
				Cured 6 Months				
1.7952	0.670	0.230	0.473	0.290	1.66	0.67	0.239	1.06
1.8249	0.645	0.230	0.460	0.272	1.75	0.68	0.276	1.29
1.8508	0.623	0.230	0.448	0.254	1.94	0.75	0.285	1.50
1.9159	0.566	0.227	0.415	0.209	2.25	0.88	0.267	1.60
1.9186	0.565	0.227	0.414	0.208	2.34	0.91	0.286	1.80
1.9227	0.560	0.227	0.410	0.203	2.42	0.95	0.268	1.73
1.9278	0.556	0.227	0.408	0.200	2.41	0.93	0.297	1.97
1.9274	0.556	0.227	0.408	0.199	2.34	0.92	0.266	1.66
2.0143	0.482	0.218	0.359	0.141	3.07	1.26	0.222	1.85
2.0296	0.467	0.218	0.344	0.123	3.14	1.21	0.290	2.50
2.0391	0.460	0.218	0.338	0.114	3.22	1.29	0.243	2.09
2.0503	0.450	0.218	0.328	0.102	3.19	1.25	0.279	2.41
				Cured 7 Months				
1.8489	0.624	0.226	0.453	0.263	2.00	0.76	0.313	1.78
1.8684	0.608	0.226	0.444	0.250	2.03	0.79	0.279	1.51
1.8868	0.591	0.226	0.433	0.235	2.15	0.84	0.280	1.19
1.9406	0.544	0.224	0.403	0.195	2.52	0.99	0.275	1.88
1.9423	0.543	0.224	0.402	0.194	2.51	1.01	0.240	1.60
1.9452	0.541	0.224	0.400	0.192	2.51	0.99	0.269	1.81
2.0445	0.457	0.216	0.338	0.114	3.26	1.26	0.291	2.59
2.0518	0.449	0.216	0.330	0.103	3.26	1.27	0.280	2.47
2.0534	0.448	0.216	0.329	0.102	3.26	1.24	0.316	2.95
				Cured 24 Months				
1.795	0.702	0.236	0.491	0.307	1.59	0.64	0.240	1.02
1.805	0.693	0.236	0.487	0.301	1.63	0.60	0.358	1.92
1.820	0.680	0.236	0.481	0.291	1.64	0.68	0.205	0.93
2.010	0.509	0.225	0.378	0.156	2.90	1.18	0.220	1.72
2.027	0.494	0.225	0.365	0.138	3.09	1.21	0.269	2.22
2.044	0.479	0.225	0.351	0.120	3.14	1.24	0.273	2.31

where

$$R_o = \frac{1 + \left(\frac{b}{a}\right)^2}{4 - 2.521\,\frac{a}{b}} \tag{5}$$

In these equations a, b, and l are the thickness, width and length, respectively, of the specimen, and T is a shape factor that is within 0.5 percent of unity for our thin-slab specimens. These calculated moduli have been converted from dynes/cm^2 to psi and included in Tables 2, 3, and 4. The uncertainty in the calculated elastic moduli was obtained from the propagation of the errors in the measured quantities. For thin slabs about 1.0 mm thick the errors in the Young's and shear moduli are about three percent. These errors are reduced as the thickness is increased.

Poisson's ratio for each thin slab was calculated from

$$\nu = \frac{E}{2G} - 1 \tag{6}$$

These values are also given in Tables 2, 3 and 4. The small errors in the resonance frequencies and dimensions combine to yield an uncertainty of about 6 percent in the values of Poisson's ratio.

Tables 2, 3, and 4 include the values of the bulk modulus, K, calculated from the theoretical relationship

$$K = \frac{EG}{3(3G - E)} = \frac{E}{3(1 - 2\nu)} \tag{7}$$

The errors in the measured quantities combine to yield an error of about 9 percent in the bulk modulus.

DISCUSSION OF RESULTS

The effect of porosity on the elastic moduli was compared with an empirical equation given by Powers (3):

$$E = E_g (1 - \epsilon_c)^3 \tag{8}$$

in which E_g is a constant. [In pastes in which all the cement is hydrated $(1 - \epsilon_c)$ is identical to the gel/space ratio used by Powers.] Figures 2, 3 and 4 show the results obtained with the tricalcium silicate, cement 15754 and cement 15366 pastes plotted against this function of the capillary porosity. The values for the shear modulus are also plotted. In these plots the origin is taken as a data point because the moduli must be zero at unit porosity. With the exception of the lowest porosity tricalcium silicate pastes, all of these points fit straight lines through the origin. It is possible that the lowest porosity tricalcium silicate pastes contained micro-flaws or cracks that are not directly observable.

When the total porosity is used instead of the capillary porosity, as with the 15366 cement data in Figure 5, a good fit to the form of Eq. 8 is also obtained. The results of Figure 5 show that

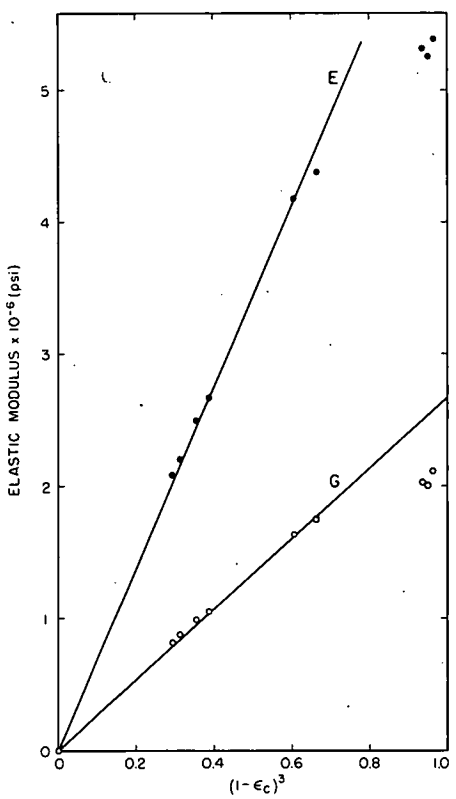

Figure 2. Elastic moduli of hardened tricalcium silicate pastes of various capillary porosities, ϵ_c.

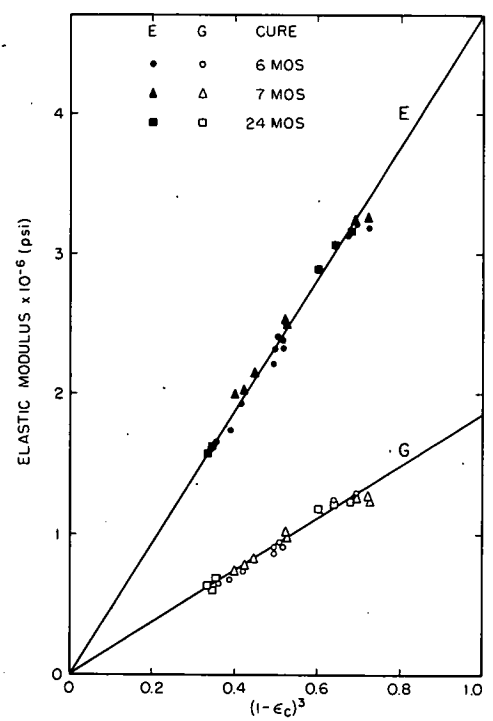

Figure 3. Elastic moduli of hardened portland cement 15754 pastes of various capillary porosities, ϵ_c, cured 6, 7 and 24 months.

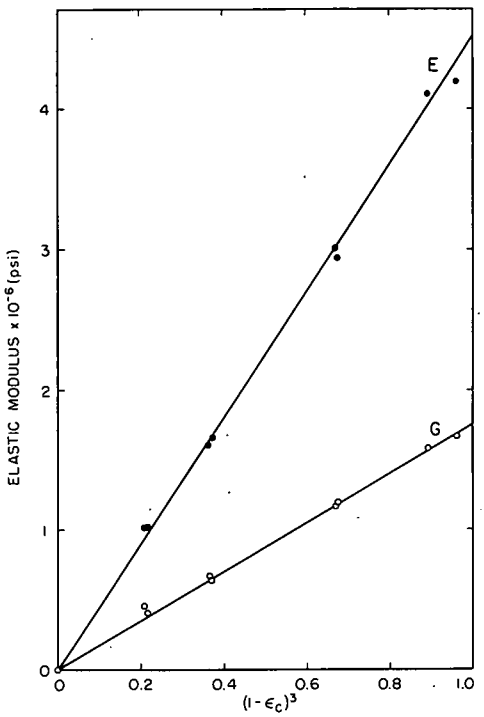

Figure 4. Elastic moduli of hardened cement 15366 pastes of various capillary porosities, ϵ_c.

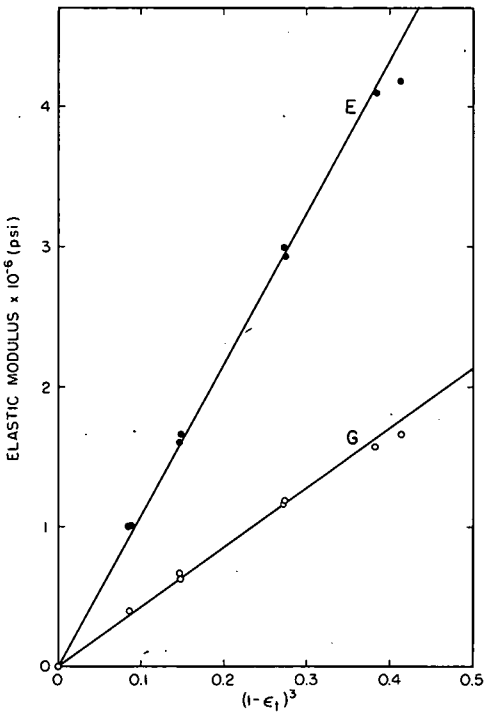

Figure 5. Elastic moduli of hardened cement 15366 pastes of various total porosities, ϵ_t.

TABLE 5

ELASTIC MODULI FOR HARDENED PASTES OF ZERO POROSITY (BY EXTRAPOLATION)

Material	Gel Phases				Solid Phases			
	$E_g \times 10^{-6}$ (psi)	$G_g \times 10^{-6}$ (psi)	$K_g \times 10^{-6}$ (psi)	ν_g	$E_1 \times 10^{-6}$ (psi)	$G_1 \times 10^{-6}$ (psi)	$K_1 \times 10^{-6}$ (psi)	ν_1
Tricalcium silicate	6.8	2.7	4.4	0.25	13.8	5.6	8.8	0.23
Cement 15366	4.5	1.75	3.4	0.28	10.8	4.3	7.9	0.27
Cement 15754	4.6	1.79	3.3	0.27	11.6	4.5	9.5	0.30

$$E = E_1(1 - \epsilon_t)^3 \qquad (9)$$

and that a similar relation applies for the shear moduli. The only value of Young's modulus of the solid phase obtainable is the value of E in Eq. 9 when the porosity is zero. Thus Young's modulus for the solid phase is E_1. Similarly Young's modulus of the gel phase, obtained from the value of E in Eq. 8 when the capillary porosity is zero, is E_g. Corresponding relationships hold for the shear moduli, G_1 and G_g. These values are listed in Table 5.

The Poisson's ratios are plotted in Figure 6 against the capillary porosity for each of three sets of data. Although the Young's and shear moduli are strongly porosity-

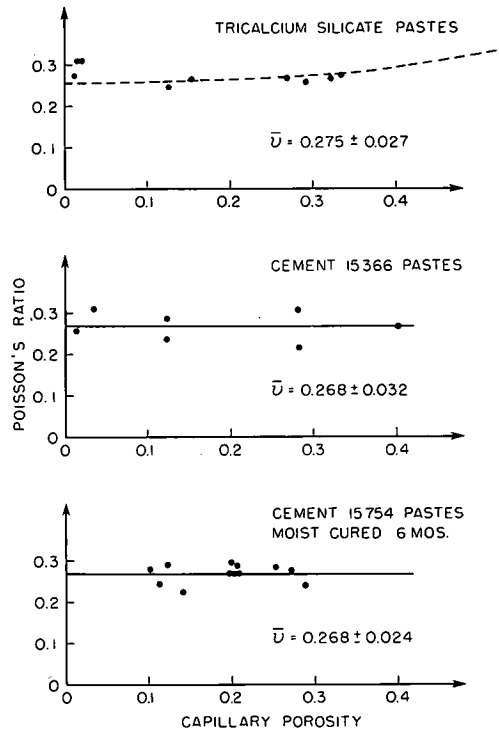

Figure 6. Poisson's ratio of hardened pastes.

dependent, the values of Poisson's ratio are not. Thus the specimens may be grouped to obtain the mean value for each set: for the tricalcium silicate paste data, $\nu = 0.275 \pm 0.021$ over the porosity range 0.21 to 0.48; for the portland cement 15366 paste data, $\nu = 0.268 \pm 0.032$ over the porosity range 0.25 to 0.56; for the portland cement 15754 paste data, $\nu = 0.271 \pm 0.032$ over the porosity range 0.33 to 0.49. The uncertainties given are the standard deviations. There was no statistically significant variation of Poisson's ratio with porosity, curing period, or composition for these sets of data.

Bulk moduli were calculated from Eq. 7. The scatter of the calculated values of K is greater than those of E and G when plotted against functions of porosity. The points for the six highest porosity tricalcium silicate pastes are fitted with a straight line by the method of least squares. The equation of the line is:

$$K = (0.25 \pm 0.13) + (4.25 \pm 0.38)(1 - \epsilon_c)^3 \quad (10)$$

in which the units of K are 10^6 psi. The three sets of cement 15754 data were grouped to yield:

$$K = (0.04 \pm 0.21) + (3.36 \pm 0.38)(1 - \epsilon_c)^3 \quad (11)$$

In these least squares analyses the origin was not regarded as a data point because the bulk modulus of the water in the pores was not zero.

Equation 10 reveals an apparent inconsistency between Eq. 7 used to calculate K, and the empirical porosity dependence of E, G, and K. If both E and G have the form of Eq. 8, then ν should be constant and the K plot should also intersect the origin. However, Eq. 10 shows that the K plot does not intersect the origin. In fact, the intercept of $(0.25 \pm 0.13) \times 10^6$ psi agrees with the bulk modulus of water at 25 C, 0.32×10^6 psi (12). This suggests that the form of Eq. 8 cannot be exactly correct for both the E and G plots. To examine this possibility, Eq. 8 for E and Eq. 10 for K were substituted in Eq. 7 and solved for ν. It was found that ν is nearly constant but increases slightly with porosity as shown by the dashed curve in Figure 6. As the porosity approaches unity, ν increases more rapidly and approaches 0.5, the value expected for a fluid. This variation of ν means that the linear dependence of the moduli on $(1 - \epsilon)^3$ cannot be exactly correct for both E and G, and may not be correct for either. The deviations from linearity, however, need not be large because ν depends only on the ratio E/G. This ratio can change considerably for large values of ϵ and account for the finite intercept for K without requiring large deviations from linearity.

If, as seems to be the case for E and G, the bulk moduli are not exactly linear in $(1 - \epsilon_c)^3$, we should not expect the intercepts of Eqs. 10 and 11 to be exactly the value for the bulk modulus of water. The value of the exactly correct function of porosity should approach the bulk modulus of water as the porosity approaches unity, but a slight curvature of the correct function would yield an intercept slightly different from that obtained from the linear fit to the data. Since the calculated intercepts are not much different from the bulk modulus of water, the $(1 - \epsilon_c)^3$ dependence appears to be highly accurate over the range of the available data.

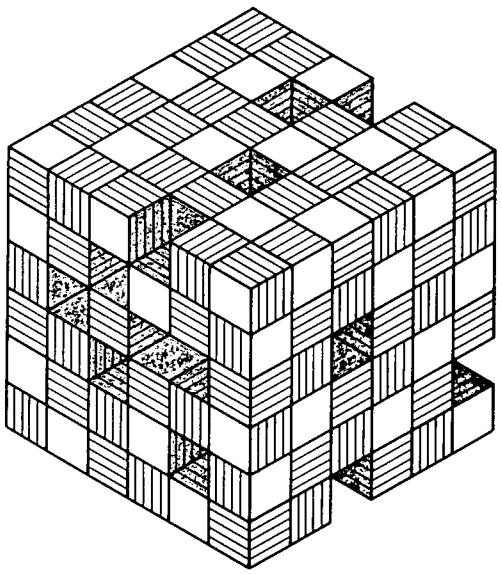

Figure 7. Stacks of thin particles regularly arranged in a porous structure.

Although Powers' Eq. 8 was introduced as a purely empirical relationship, a basis for it can be found in a simple model of paste structure. Let us consider the properties of a model of paste structure constructed by bonding together identical stacks of thin sheet-like tobermorite gel particles (2). For simplicity, let us take the stacks to be cubes and build the structure by stacking up the cubes in a regular way. To insure that the model will have identical properties in each principal direction let us orient the stacks so that one third of the stacks are oriented in each of the three principal directions. Let us assume that the average strain in the stacks is equal to the average strain in the structure. Porosity may be introduced by removal of some of the stacks, as shown in Figure 7. If the porosity of such a structure is regarded as the capillary porosity, ϵ_c, and if the structure is only one layer of stacks thick, the Young's modulus is reduced according to

$$E(1) = E_{avg}(1 - \epsilon_c) \qquad (12)$$

To determine the effective modulus of structures consisting of many layers of stacks, we need only consider how a layer of stacks interacts with other layers in the structure. Consider the nth layer of stacks in a structure during (vertical) compression of the structure. If there are no pores (missing stacks) and the principal moduli are nearly equal, the stress is essentially uniform. If there are pores the stress must be carried by stacks adjacent to the pores so that there is a concentration of stress around each pore. At some distance from each pore the stress becomes essentially uniform. Between the pore and the region of uniform stress there is a region of solid which carries little or none of the stress. Let us approximate each region of transition from no stress to uniform stress by a step-function which varies from zero to the average stress at a distance of one stack from the pore. This is equivalent to assuming that the presence of the pore makes the stacks immediately above and below the pore completely ineffective in carrying stress, but has no effect at greater distances.

Now since each stack in the nth layer has a probability of $(1 - \epsilon_c)^2$ of being in contact with an occupied site in both the (n + 1) st layer and the (n - 1) st layer, the effective modulus is reduced to

$$E = E_{avg}(1 - \epsilon_c)^3 \qquad (8a)$$

Hence the empirically found porosity dependence may be simply related to confining the elastic interactions of stacks in the model to nearest-neighbor interactions of either zero or average stress.

Even if the stacks are not strongly bonded to each other, stacks can bridge around the pores if the stacks are not so regularly arranged as in Figure 7. If the stacks are displaced so as to overlap the stacks in adjacent layers, then bridging around pores can occur even without strong bonding of the stacks.

If the porosity of the stacks is now added to the capillary porosity to obtain the total porosity of each layer of stacks, the argument used to obtain Eq. 12 may be repeated with the same result, except that the total porosity is used instead of the capillary porosity. Since the pore size distribution curves for cement pastes are continuous functions and the definition of the gel porosity is somewhat arbitrary, there seems to be no reason to distinguish between the gel pores and capillary pores when the total porosity is used (13).

ACKNOWLEDGMENTS

The authors gratefully acknowledge the assistance of other members of the staff of the Portland Cement Association Laboratories. The authors would also like to express their indebtedness to Dr. T. C. Powers, whose persistent search for truth and order has served as an example and inspiration for us all.

REFERENCES

1. Powers, T. C. Physical Properties of Cement Paste. Fourth Internat. Symposium on Chem. of Cement, Washington, 1960. Proc., Vol. 2, pp. 577-609; PCA Res. Dept. Bull. 154.
2. Brunauer, S., and Greenberg, S. A. The Hydration of Tricalcium Silicate and β-Dicalcium Silicate at Room Temperature. Fourth Internat. Symposium on Chem. of Cement, Washington, 1960. Proc., Vol. 1, pp. 135-165; PCA Res. Dept. Bull. 152.
3. Powers, T. C. Fundamental Aspects of Shrinkage of Concrete. Revue des Materiaux, No. 544, pp. 79-85, 1961.
4. Hansen, T. C. Influence of Aggregate and Voids on Modulus of Elasticity of Concrete, Cement Mortar, and Cement Paste. Jour. ACI (Proc.), Vol. 62, pp. 193-216, 1965.
5. Hashin, Z. The Elastic Moduli of Heterogeneous Materials. Jour. Appl. Mech., Vol. 29-E, pp. 143-150, 1962.
6. ASTM Designation C-204-55.
7. Powers, T. C., Copeland, L. E., Hayes, J. C., and Mann, H. M. Permeability of Portland Cement Paste. Jour. ACI (Proc.), Vol. 51, pp. 285-300, 1954; PCA Res. Dept. Bull. 53.
8. Powers, T. C. The Bleeding of Portland Cement Paste, Mortar, and Concrete. PCA Res. Dept. Bull. 2, p. 88, 1939.
9. Copeland, L. E., and Hayes, J. C. The Determination of Non-Evaporable Water in Hardened Portland Cement Paste. ASTM Bull. 194, 1953; PCA Res. Dept. Bull. 47.
10. Copeland, L. E., and Hayes, J. C. Porosity of Hardened Portland Cement Pastes. Jour. ACI (Proc.), Vol. 52, pp. 633-640, 1956; PCA Res. Dept. Bull. 68.
11. Spinner, S., and Tefft, W. E. A Method for Determining Mechanical Resonance Frequencies and for Calculating Elastic Moduli from These Frequencies. ASTM Proc., Vol. 61, pp. 1221-1238, 1961.
12. Lindsay, Robert. Density and Compressibility of Liquids. American Institute of Physics Handbook, p. 2-175, McGraw-Hill, New York, 1963.
13. Mikhail, R. Sh., Copeland, L. E., and Brunauer, S. Pore Structures and Surface Areas of Hardened Portland Cement Pastes by Nitrogen Adsorption. Can. Jour. Chem., Vol. 42, pp. 426-438, 1964; PCA Res. Dept. Bull. 167.